Extended asymmetric-cut multilayer X-ray gratings

Mauro Prasciolu,[1] Anton Haase,[2] Frank Scholze,[2] Henry N. Chapman,[3,4] and Saša Bajt[1,*]

[1]*Photon Science, DESY, Notkestrasse 85, Hamburg, 22607, Germany*
[2]*Physikalisch-Technische Bundesanstalt, Abbestrasse 2-12, Berlin, 10587, Germany*
[3]*Center for Free-Electron Laser Science, DESY, Notkestrasse 85, Hamburg, 22607, Germany*
[4]*Department of Physics, University of Hamburg, Luruper Chaussee 149, Hamburg, 22761, Germany*
[*]*sasa.bajt@desy.de*

Abstract: The fabrication and characterization of a large-area high-dispersion blazed grating for soft X-rays based on an asymmetric-cut multilayer structure is reported. An asymmetric-cut multilayer structure acts as a perfect blazed grating of high efficiency that exhibits a single diffracted order, as described by dynamical diffraction throughout the depth of the layered structure. The maximum number of grating periods created by cutting a multilayer deposited on a flat substrate is equal to the number of layers deposited, which limits the size of the grating. The size limitation was overcome by depositing the multilayer onto a substrate which itself is a coarse blazed grating and then polish it flat to reveal the uniformly spaced layers of the multilayer. The number of deposited layers required is such that the multilayer thickness exceeds the step height of the substrate structure. The method is demonstrated by fabricating a 27,060 line pairs per mm blazed grating (36.95 nm period) that is repeated every 3,200 periods by the 120-μm period substrate structure. This preparation technique also relaxes the requirements on stress control and interface roughness of the multilayer film. The dispersion and efficiency of the grating is demonstrated for soft X-rays of 13.2 nm wavelength.

OCIS codes: (050.1950) Diffraction gratings; (050.7330) Volume gratings; (340.7480) X-rays, soft x-rays, extreme ultraviolet (EUV).

References and links

1. V. E. Levashov and A. V. Vinogradov, "Resonance diffraction efficiency enhancement in sliced multilayers," Appl. Opt. **32**(7), 1130–1135 (1993).
2. R. M. Fechtchenko, A. V. Vinogradov, and D. L. Voronov, "Optical properties of sliced multilayer gratings," Opt. Commun. **210**(3-6), 179–186 (2002).
3. S. Bajt, H. N. Chapman, A. Aquila, and E. Gullikson, "High-efficiency x-ray gratings with asymmetric-cut multilayers," J. Opt. Soc. Am. A **29**(3), 216–230 (2012).
4. X. Yang, I. V. Kozhevnikov, Q. Huang, and Z. Wang, "Unified analytical theory of single order soft x-ray multilayer gratings," J. Opt. Soc. Am. B **32**(4), 506–522 (2015).
5. E. Spiller, "Reflective multilayer coatings for the far uv region," Appl. Opt. **15**(10), 2333–2338 (1976).
6. J. C. Rife, W. R. Hunter, T. W. Barbee, Jr., and R. G. Cruddace, "Multilayer-coated blazed grating performance in the soft x-ray region," Appl. Opt. **28**(15), 2984–2986 (1989).
7. P. P. Naulleau, J. A. Liddle, E. H. Anderson, E. M. Gullikson, P. Mirkarimi, F. Salmassi, and E. Spiller, "Fabrication of high-efficiency multilayer-coated gratings for the EUV regime using e-beam patterned substrates," Opt. Commun. **229**(1–6), 109–116 (2004).
8. D. L. Voronov, E. H. Anderson, R. Cambie, S. Cabrini, S. D. Dhuey, L. I. Goray, E. M. Gullikson, F. Salmassi, T. Warwick, V. V. Yashchuk, and H. A. Padmore, "A 10,000 groove/mm multilayer coated grating for EUV spectroscopy," Opt. Express **19**(7), 6320–6325 (2011).
9. D. L. Voronov, R. Cambie, R. M. Feshchenko, E. M. Gullikson, H. A. Padmore, A. V. Vinogradov, and V. V. Yashchuk, "Development of an ultra-high resolution diffraction grating for soft X-rays," Proc. SPIE **6705**, 67050E (2007).

#237670 - $15.00 USD Received 7 Apr 2015; revised 25 May 2015; accepted 26 May 2015; published 1 Jun 2015

10. D. L. Voronov, R. Cambie, E. M. Gullikson, V. V. Yashchuk, H. A. Padmore, Y. P. Pershin, A. G. Ponomarenko, and V. V. Kondratenko, "Fabrication and characterization of a new high density Sc/Si multilayer sliced grating," Proc. SPIE **7077**, 707708 (2008).
11. D. L. Voronov, E. H. Anderson, E. M. Gullikson, F. Salmassi, T. Warwick, V. V. Yashchuk, and H. A. Padmore, "Ultra-high efficiency multilayer blazed gratings through deposition kinetic control," Opt. Lett. **37**(10), 1628–1630 (2012).
12. D. L. Voronov, E. M. Gullikson, F. Salmassi, T. Warwick, and H. A. Padmore, "Enhancement of diffraction efficiency via higher-order operation of a multilayer blazed grating," Opt. Lett. **39**(11), 3157–3160 (2014).
13. V. Ayvazyan, N. Baboi, J. Bähr, V. Balandin, B. Beutner, A. Brandt, I. Bohnet, A. Bolzmann, R. Brinkmann, O. I. Brovko, J. P. Carneiro, S. Casalbuoni, M. Castellano, P. Castro, L. Catani, E. Chiadroni, S. Choroba, A. Cianchi, H. Delsim-Hashemi, G. Di Pirro, M. Dohlus, S. Düsterer, H. T. Edwards, B. Faatz, A. A. Fateev, J. Feldhaus, K. Flöttmann, J. Frisch, L. Fröhlich, T. Garvey, U. Gensch, N. Golubeva, H.-J. Grabosch, B. Grigoryan, O. Grimm, U. Hahn, J. H. Han, M. V. Hartrott, K. Honkavaara, M. Hüning, R. Ischebeck, E. Jaeschke, M. Jablonka, R. Kammering, V. Katalev, B. Keitel, S. Khodyachykh, Y. Kim, V. Kocharyan, M. Körfer, M. Kollewe, D. Kostin, D. Krämer, M. Krassilnikov, G. Kube, L. Lilje, T. Limberg, D. Lipka, F. Löhl, M. Luong, C. Magne, J. Menzel, P. Michelato, V. Miltchev, M. Minty, W. D. Möller, L. Monaco, W. Müller, M. Nagl, O. Napoly, P. Nicolosi, D. Nölle, T. Nuñez, A. Oppelt, C. Pagani, R. Paparella, B. Petersen, B. Petrosyan, J. Pflüger, P. Piot, E. Plönjes, L. Poletto, D. Proch, D. Pugachov, K. Rehlich, D. Richter, S. Riemann, M. Ross, J. Rossbach, M. Sachwitz, E. L. Saldin, W. Sandner, H. Schlarb, B. Schmidt, M. Schmitz, P. Schmüser, J. R. Schneider, E. A. Schneidmiller, H.-J. Schreiber, S. Schreiber, A. V. Shabunov, D. Sertore, S. Setzer, S. Simrock, E. Sombrowski, L. Staykov, B. Steffen, F. Stephan, F. Stulle, K. P. Sytchev, H. Thom, K. Tiedtke, M. Tischer, R. Treusch, D. Trines, I. Tsakov, A. Vardanyan, R. Wanzenberg, T. Weiland, H. Weise, M. Wendt, I. Will, A. Winter, K. Wittenburg, M. V. Yurkov, I. Zagorodnov, P. Zambolin, and K. Zapfe, "First operation of a free-electron laser generating GW power radiation at 32 nm wavelength," Eur. Phys. J. D **37**(2), 297–303 (2006).
14. P. Philippe, S. Valette, O. M. Mendez, and D. Maystre, "Wavelength demultiplexer: using echelette gratings on silicon substrate," Appl. Opt. **24**(7), 1006–1011 (1985).
15. C. Laubis, A. Fischer, and F. Scholze, "Extension of PTB's EUV metrology facilities," Proc. SPIE **8322**, 832236 (2012).
16. J. Tümmler, H. Blume, G. Brandt, J. Eden, B. Meyer, H. Scherr, F. Scholze, and G. Ulm, "Characterization of the PTB EUV reflectometry facility for large EUVL optical components," Proc. SPIE **5037**, 482668 (2003).
17. S. E. Bae, M. K. Oh, N. N. Min, S.-H. Paek, S. I. Hong, and C. W. J. Lee, "Preparation of atomically flat Si(111)-H surfaces in aqueous ammonium fluoride solutions investigated by using electrochemical, in situ EC-STM and ATR-FTIR spectroscopic methods," Bull. Korean Chem. Soc. **25**(12), 1822–1828 (2004).
18. R. E. Oosterbroek, J. W. Berenschot, H. V. Jansen, A. J. Nijdam, G. Pandraud, A. Van den Berg, and M. C. Elwenspoek, "Etching methodologies in <111> oriented silicon wafers," J. Microelectromech. Syst. **9**(3), 390–398 (2000).
19. P. B. Mirkarimi, S. Bajt, and M. A. Wall, "Mo/Si and Mo/Be multilayer thin films on Zerodur substrates for extreme-ultraviolet lithography," Appl. Opt. **39**(10), 1617–1625 (2000).

1. Introduction

Asymmetric-cut multilayers are volume diffraction elements that act as gratings. Angular dispersion of the Bragg-reflected beam is caused by the asymmetric truncation of the multilayer stack [1–3]. In a recent paper [4] a unified analytical theory of single-order soft x-ray multilayer gratings was presented, that can be applied to different multilayer gratings including asymmetric-cut multilayer gratings discussed here. The condition for diffraction of the X-ray beam of wavelength λ is that it satisfies the Bragg condition in the multilayer film, that is

$$m\lambda = 2d\sin\theta_B \tag{1}$$

where d is the multilayer period and θ_B is the Bragg angle of reflection. For a cut of the multilayer of included angle γ between the new surface and the layers, a period of $D = d/\sin\gamma$ is revealed at the cut surface. Since the layers in the structure are not parallel to the surface (due to the asymmetric cut) the Bragg reflection does not have equal angles of incidence and reflection relative to the surface. However, setting $d = D\sin\gamma$ in Eq. (1) recovers the grating equation

$$m\lambda = 2D\sin\gamma\sin\theta_B = D(\sin\beta - \sin\alpha) \tag{2}$$

#237670 - $15.00 USD Received 7 Apr 2015; revised 25 May 2015; accepted 26 May 2015; published 1 Jun 2015

where $\theta_B = \pi/2 - \alpha - \gamma = \pi/2 + \gamma - \beta$ for an incidence angle α and reflected angle β, as shown in Fig. 1. The cut multilayer can be thought of as a blazed grating of period D and blaze angle γ with an over-coated multilayer structure that satisfies the Bragg condition for reflection from the facets of the blaze. The multilayer period is exactly equal to the step height of this fictional grating and so the first layer on one facet would merge seamlessly with the second layer on the neighbouring facet, and so on. In the extreme ultraviolet (EUV) to soft-X-ray regime, as compared with actually over-coating a blazed grating of period D with a multilayer of layer period d [5–8], an asymmetric-cut multilayer more closely resembles an ideal volume grating structure and hence can be more efficient.

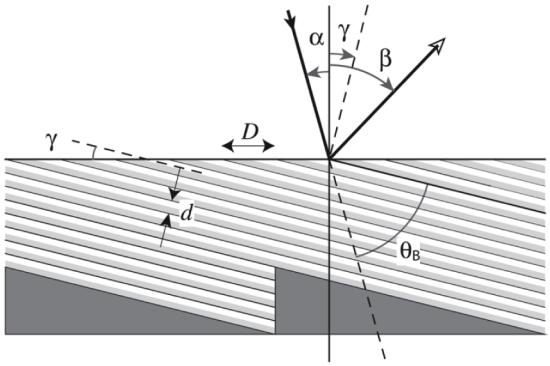

Fig. 1. Geometry of diffraction from a blazed grating. We use the convention that incidence and diffracted rays on opposite sides of the surface normal have angles α and β of the same sign. The blaze angle is γ, not to be confused with the multilayer Bragg angle θ_B.

Asymmetric-cut multilayers can be prepared by depositing layers onto a flat substrate and then cutting or slicing this coating under an angle to reveal the underlying layers. Through sputtering, it is possible to achieve layer periods in the range of several ångströms to tens of nanometres with a correspondingly high precision. This translates into grating periods of the cut multilayer of similar dimensions and precision. For example, a multilayer of 1 nm period cut at an angle of 10° from the plane of the surface will result in an effective grating period of 5.8 nm (174,000 line pairs per mm). It has been previously demonstrated that the performance of asymmetric-cut layered structures are indeed indistinguishable from a perfect blazed grating [3], with only a single on-blaze diffracted order that can be measured for a given wavelength and incidence angle, and no discernable zero order reflection. This compares with ruled gratings that often exhibit diffracted power in multiple off-blaze angles, including the zero order.

Asymmetric-cut multilayer structures are novel optical elements that can be used in different applications, such as monochromators, spectrometers and pulse compressors. In general one needs to maximize the number of periods when higher spectral resolution is needed. This also requires perfect multilayer periodicity from the top to the bottom of the multilayer stack since any drift in deposition rate will lead to an accumulating error in the grating structure. If the stress from the thick multilayer stack is too high it can result in substrate bending, cracking or even delamination of the multilayer from the substrate. Another issue of concern is accumulated roughness that lowers the grating reflectivity and efficiency. Nevertheless, in addition to achieve higher spectral resolution, asymmetric-cut multilayer gratings with thousands of periods (larger areas) are required to accommodate large beams or to avoid radiation damage. For example, if the gratings are used as part of a pulse compressor, multiple (two to four) gratings must be placed in a large area unfocused free electron laser (FEL) beam. The dispersed beam from the first grating must be captured by a second and possibly third and fourth gratings that are, at least, as large as that beam.

#237670 - $15.00 USD Received 7 Apr 2015; revised 25 May 2015; accepted 26 May 2015; published 1 Jun 2015

One method to overcome the limitation of the number of achievable periods in a grating was proposed [9] and demonstrated [10] in which a small period, shallow blazed grating substrate was over-coated with a multilayer. Scanning beam interference lithography combined with anisotropic KOH etching of a silicon single crystal was used to prepare smooth blazed grating substrates. These were over-coated with a 40 bilayer Sc/Si multilayer of a total thickness < 150 nm. In more recent work Mo/Si multilayers consisting of 30 bilayers were used to overcoat a grating with a period of 190 nm and a blaze angle of 2°. The depth of triangular grooves in the direction perpendicular to the blazed facets (6.63 nm) almost perfectly matched the multilayer period of 6.7 nm. A grating with 5,250 lines per mm groove density had an efficiency of 44% in the first order with none of the higher orders exceeding 1% [11] while more recently 52% efficiency in the second order was achieved [12] with a blazed grating with 2,525 lines per mm groove density. With this approach the x-ray dispersion is limited by the groove density of the blazed grating substrate and multilayer is used only to increase the reflectivity.

In this paper we present a new development based on previously demonstrated asymmetric-cut multilayer structures [3] but going beyond the above-mentioned limitations. We use layer deposition as a way to produce grating periods much smaller than possible by other means. This way we achieved almost three times higher grating frequency (27,060 lines per mm vs. 10,000 lines per mm [8]) than previously reported.

2. Experimental details

To fabricate a grating with a large number of periods that exceeds deposition limits we developed a method of depositing a multilayer on a coarse blazed grating substrate followed by planarization of the top surface. We produced the underlying blazed grating substrate by anisotropic wet etching of an asymmetric-cut single-crystal silicon such that the Si {111} planes were not parallel to the surface but inclined at the blaze angle required for the final grating. By using an etchant that etches >25 times faster in the <100> crystal direction than in the <111> direction we exposed faces of {111} planes to the surface. Etching proceeds by predominantly removing material along {111} planes but not perpendicular to them. Hence, a lined structure that is formed on the surface and which is impervious to etching creates {111} surface facets if the lined structure is perpendicular to the asymmetric cut angle, as shown in Fig. 2. A substrate blazed grating structure was created by using an etchant mask that consists of lines that are much thinner than the period of that grating (i.e. a low duty cycle) and which themselves were aligned perpendicular to the cut angle. This process exposes {111} facets that slightly undercut the mask at the step. The substrate grating was then obtained by removing the etch stop structure and the nubs (tiny ridges of silicon) that remain from the undercutting. This was then used as a substrate for the multilayer coating.

For an experiment at Free electron LASer facility at Hamburg (FLASH) [13] we produced a grating with 27,060 lines per mm and a 10.5° blaze angle for soft X-rays of 13.2 nm wavelength. Our gratings were rectangular (16 mm x 9 mm) and each piece was formed on a blazed grating substrate with about 133 periods. The blazed grating substrate had a pitch of 120 μm. The blazed grating substrate was coated with a Mo/Si multilayer of 6.7 nm period and a total thickness of 22 μm prior to planarization.

Custom cut silicon {111} wafers with 10.5° off-axis angle were obtained from Silicon Valley Microelectronics. The wafers had a 200 nm thick thermal silicon dioxide coating, which acted as the etchant stop in our procedure. The direction of the cut was indicated by a flat edge of the wafer, referred to as the "flat reference", within an error of ± 0.5°. The etching procedure started by coating a wafer with 500 nm thick positive photoresist (AZ1505). Our pattern to be etched consisted of 3 μm wide lines, spaced by the grating pitch of 120 μm (a duty cycle of 2.5%) that was printed on a binary photomask. This pattern was then transferred into photoresist using a mask aligner (MJB4, SUSS MicroTec). After developing the resist using AZ351B developer, the pattern was transferred into the thermal silicon dioxide layer by

#237670 - $15.00 USD Received 7 Apr 2015; revised 25 May 2015; accepted 26 May 2015; published 1 Jun 2015

wet etching in Buffered Etch Oxide (BOE 7:1) solution. The resulting surface silicon dioxide structure consisted of 3 μm wide lines that formed the etch stop for the anisotropic silicon etching, which was carried out by wet etching in Tetramethyl-ammonium hydroxide (TMAH) solution 25% in water at 75°C for 45 minutes.

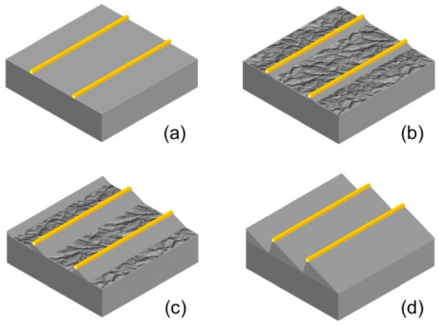

Fig. 2. Schematic overview of the anisotropic wet etching steps. (a) Mask transfer onto photoresist; (b) and (c) progressive etching along desired crystallographic direction; and (d) final blazed grating substrate with smooth surface.

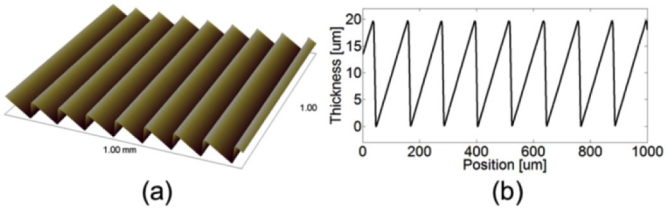

Fig. 3. A 3D topology map (a) and a line scan in cross section (b) of the blazed grating substrate prior to multilayer coating, as measured with a profilometer.

The precision to which we need to orient lines to be perpendicular to the cut direction of the wafer depends on the grating line length. If the error is too large we obtain an increased undercut of the lines and an increased dead area between facets where the etched surface is not parallel to the {111} planes. For our application with a grating line length of 20 mm, we needed to find the cut direction to within 0.1°, which exceeded the confidence given by the reference flat. We therefore determined the cut direction by initial etching trials using a fan pattern of lines that was included on the photomask. The fan pattern consisted of 51 lines (1 μm wide and 3 mm long) of equally spaced orientations ranging from –2.5° to 2.5° relative to the expected direction. By inspecting the pattern on the wafer with a microscope after anisotropic wet etching we could determine the line orientation with the least degree of undercut. In this way we determined the in-plane direction of the cut to an angular resolution of 0.1°, and used it to orient the 120 μm-pitch lines on subsequent wafers of the same batch. After the anisotropic silicon etching the top part of the groove structures exhibited a nub due to the mask undercutting. The nub structures were rounded by over-etching the substrate in TMAH for 90 seconds after the silicon dioxide mask removal in BOE [14]. A schematic overview of the blazed substrate fabrication process is presented in Figs. 2(a)-2(d). Blazed substrates were examined by optical microscopy and measured with a profilometer (Fig. 3) and an atomic force microscope (AFM).

The resulting substrate blazed grating structures [Fig. 4(a)] were then inserted in our magnetron sputtering deposition system (up to four at a time) and over-coated with a Mo/Si multilayer consisting of 3,200 bilayers of 6.7 nm period, with $\Gamma = 0.5$ ($\Gamma \equiv d_{Mo}$ / period) (Fig. 3). Each substrate was mounted on a rotating platter, which transported them across the sputtering sources arranged along a circular path. The transverse thickness profile of the

#237670 - $15.00 USD Received 7 Apr 2015; revised 25 May 2015; accepted 26 May 2015; published 1 Jun 2015

deposited layers was controlled by modulating the platter velocity. Deposition was performed using ultrapure (99.9999%) Ar sputtering gas at 0.182 Pa and large magnetron sources (127 mm × 254 mm) in a DC power controlled mode of 360 W (Si) and 180 W (Mo). Thin Mo/Si multilayers (with 35 bilayers) were deposited on flat Si wafers under the same conditions before and after the thick-multilayer coating of the blazed substrates. These witness samples were used to measure changes in period thickness due to target consumption since depositions of 3,200 bilayer multilayers each took over 25 hours.

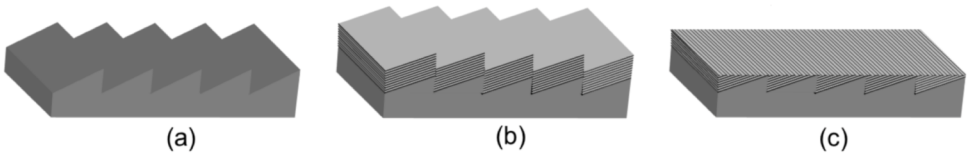

Fig. 4. Steps to fabricate an extended asymmetric-cut multilayer X-ray grating: (a) prepare smooth blazed grating substrate; (b) overcoat it with a thick periodic multilayer, thicker than the grating step heights; and (c) remove the excess material by polishing the top surface flat to reveal the asymmetric-cut multilayer that acts as a grating.

The multilayer period and interface roughness of the flat witness samples were determined from measurements with an X-ray diffractometer (X'Pert Pro, Panalytical) using Cu K-alpha X-rays at grazing incidence. These revealed that the sputter rate did not change by more than 0.4% during the whole deposition run. The high spatial frequency roughness of the surface of the witness samples and coated grating was measured with an AFM (Dimension Icon, Bruker). The multilayer structures on the blazed grating substrates were investigated in cross section by scanning electron microscope of sections prepared with a focused ion beam (FIB, FEI Helios Nanolab).

After multilayer coating of the blazed grating structure [Fig. 4(b)] the top surface was made flat [Fig. 4(c)] using a mechanical polishing device (Ultrapol, Ultra Tec) with controllable sample angle, load, polishing speed and time. During the polishing we frequently inspected the sample with an optical microscope so that we could stop polishing before reaching the silicon tips of the underlying substrate. The finely polished surface, which exhibits the asymmetric-cut multilayer structure, was also inspected with an AFM.

The grating's dispersion and efficiency was measured at the EUV radiometry beamline located at Physikalisch-Technische Bundesanstalt's (PTB)'s own electron storage ring "Metrology Light Source" [15,16]. It uses a plane grating monochromator, which covers the spectral range from 5 nm to 50 nm. Reflectivity measurements were made with a 10 × 10 mm^2 GaAs X-ray diode detector mounted on a movable arm and located at 154 mm from the sample. The dispersion (maps of reflectivity as a function of detector angle and wavelength) was measured with a 4.5 × 1.0 mm^2 aperture placed in front of the diode with the diode at the largest distance of 550 mm from the grating.

3. Results and discussion

We start our discussion with the effect of the initial substrate roughness on the final multilayer structure. The blazed grating substrate prepared by wet anisotropic etching should result in a structure with atomically smooth facets [17,18]. However, our substrates have on average 0.36 ± 0.02 nm rms high-spatial-frequency roughness, which can be explained by the imperfect alignment of the mask to the crystal orientation of the substrate. Hence, our substrates were not atomically smooth. Previous studies [19] showed that the initial substrate roughness plays a role in the final multilayer reflectivity. Indeed, those studies showed that the reflectivity is inversely proportional to the initial substrate roughness. For example, a multilayer coated on a substrate with an initial roughness of 0.36 nm rms had ~10% lower reflectivity as compared to a multilayer deposited on a substrate with an initial roughness of 0.12 nm rms. In addition, multilayer roughness after the coating was compared with the initial

#237670 - $15.00 USD Received 7 Apr 2015; revised 25 May 2015; accepted 26 May 2015; published 1 Jun 2015

substrate roughness. For example, a multilayer grown on a rougher substrate (0.36 nm rms) had no contribution to the final roughness. However, multilayers grown on smoother substrates (<0.36 nm rms) always increased the final roughness; the smoother the substrate the larger the contribution from the multilayer to the final roughness. In the aforementioned work substrates with an initial surface roughness between 0.06 and 0.36 nm rms were studied. However, the multilayers consisted of only 40-50 bilayers with the total multilayer thickness of 0.27 μm. This is a hundred times thinner than the multilayers used in our study (22 μm). To distinguish between the effect of the initial substrate roughness and the intrinsic multilayer roughness we deposited a 22 μm thick multilayer on a super-polished flat Si wafer (0.12 nm rms), and on the blazed grating substrate (0.36 nm rms). According to the aforementioned study a thin multilayer is expected to increase the roughness only if deposited on a very smooth substrate (e.g. 0.12 nm rms). The result for the case of a thick multilayer is not obvious. Our experimental data shows that coating a thick multilayer (22 μm) either on a smooth (0.12 nm) or on a rough (0.36 nm) substrate increases the roughness. The final roughness on the super-smooth substrate was 0.4 nm rms and on the rougher blazed grating substrate 0.45 - 0.6 nm rms. Figure 5 shows the power spectral density (PSD) spectra of these various surfaces. While the surface roughness of the multilayer deposited on an anisotropic etched Si substrate matches the initial substrate roughness almost in the whole measured frequency range [Fig. 5(a)] the multilayer deposited on super-smooth Si substrate matches the substrate only in the frequency range between 7 and 800 μm^{-1} [Fig. 5(b)]. In the lower frequency region, between 0.7 to 7 μm^{-1}, the multilayer roughness is substantially increased as compared to the initial substrate roughness.

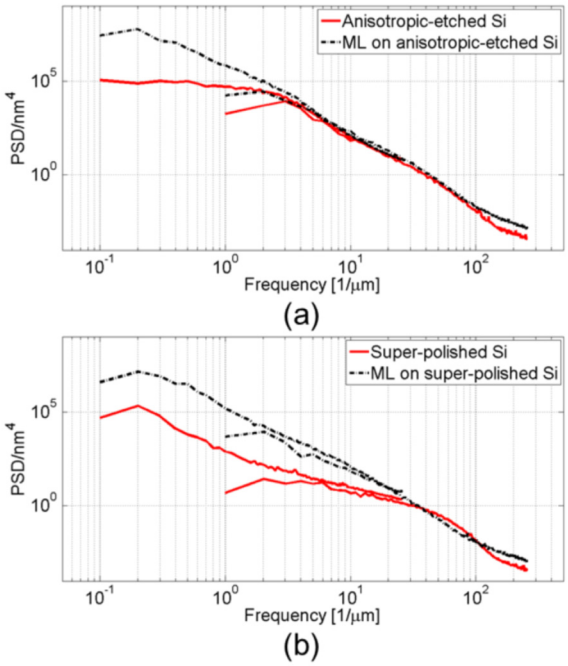

Fig. 5. (a) Power Spectral Density (PSD) spectra of an anisotropic-etched Si substrate (blazed grating substrate), bare and after coating it with 22 μm thick multilayer and (b) PSD of super-polished Si substrate with initial roughness of ~0.12 nm rms, bare and after coating it with the same thickness multilayer

Due to the inclined angle of the blazed facets of the substrate grating the reflectivity peak of the deposited multilayer is at 13.2 nm as measured along the normal of those facets compared with 13.45 nm obtained on a flat substrate that was coated during the same time.

#237670 - $15.00 USD Received 7 Apr 2015; revised 25 May 2015; accepted 26 May 2015; published 1 Jun 2015

The reflectivity of latter multilayer was also much higher (50% vs. 37.5%) as compared to the reflectivity of the multilayer coated on the blazed grating substrate. Both multilayers grown on different substrates during the same deposition run show similar PSD spectra and the roughness growth is in accordance with the trend found in reference [19]. We thus expect the reduction in reflectivity due to multilayer roughness to be about the same. The observed difference in reflectivity can instead be ascribed to a "dead area" near the substrate steps where the multilayer does not conform to the substrate and hence does not fulfill the Bragg condition, as discussed below. We estimate that the length of the "dead area" per 120 μm period can be as large as 20 μm or about 17%.

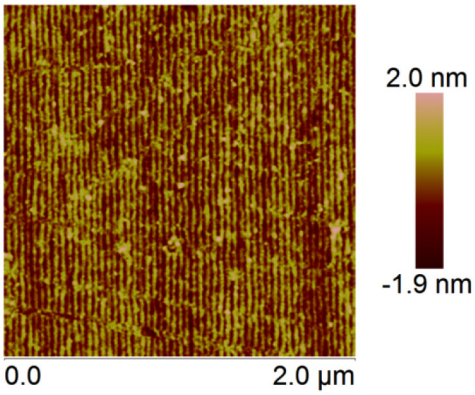

Fig. 6. A 2 × 2 μm^2 AFM image of the top asymmetric-cut multilayer surface after mechanical polishing with a surface roughness of 0.55 nm. The exposed multilayer period is 37 nm.

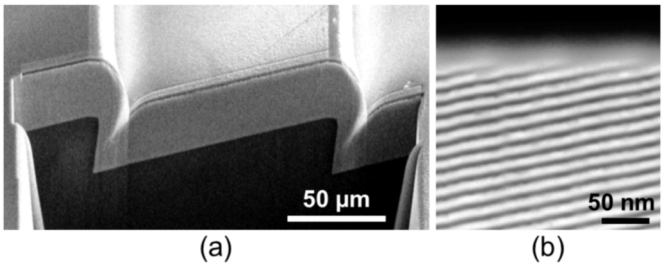

Fig. 7. (a) A cross section SEM image taken in the vicinity of one of the substrate steps of the unpolished structure. The substrate with steps height of 21.2 μm was coated with a 22 μm thick multilayer. The region on the step has noticeably thinner multilayer coating (light gray). (b) A high resolution SEM image showing individual Mo and Si layers near the top surface of the grating after polishing, in a region far away from the step. The light coloured, diffuse layer on the top surface is an amorphous layer of carbon, deposited with FIB, to protect the multilayer during the sectioning process.

After flattening the surface structure the asymmetric-cut multilayer was measured again with an AFM (Fig. 6). Polishing enhanced the topography of Mo and Si layers. This is expected since Mo and Si react differently when exposed to the air. The AFM image shown in Fig. 6 is one of several randomly chosen areas that were measured. Although occasional defects and scratches due to polishing are seen, the layers are in general relatively straight and uniform in period thickness. However, since X-rays interact with layers within the depth of the structure, the effect of these surface defects should be small as pointed out previously [3].

The SEM analysis of the sectioned multilayer revealed a high quality of the polished structure. The multilayer coating in the vicinity of one of the steps is shown in Fig. 7(a). The multilayer conforms well to the substrate on the flat part of the facet but is much thinner on the steep part of the step where the Mo and Si layers could not be seen as separate layers. We

#237670 - $15.00 USD Received 7 Apr 2015; revised 25 May 2015; accepted 26 May 2015; published 1 Jun 2015

postulate that in this region the Mo and Si layers inter-diffused and formed molybdenum silicide. In fact, a region of about 20 μm seems to be affected by this steep transition. Figure 7(b) shows a high resolution SEM image of the section of the top layers (after the 3,200 bilayer multilayer has been polished), away from the step region. There the layers are smooth, have sharp interfaces and have an angle of 10.5° to the top polished surface.

After mechanical polishing the reflectivity dropped from 37.5% to 29.7% (Fig. 8). In comparison, mechanical polishing, followed by ion-beam polishing of a multilayer deposited on a flat substrate [3] reduced the reflectivity by only a few percent. The bigger reflectivity drop observed on the grating may be due to the difference in polishing processes. It is also interesting to consider the coherence of the grating heights of the individual substrate periods, which depends on how accurately the substrate steps can be etched. If the mask is imperfect or the substrate is not perfectly flat prior to etching (as we postulate here) the step height is not constant to within a fraction of a multilayer period. Errors will cause phase offsets from one substrate period to the next. The grating structure can be described as a perfect grating modulated by regularly spaced phase steps of random heights, which will give rise to a diffraction order given by that of the perfect grating convolved with the Fourier transform of the function of phase steps. For random phase step errors this transform will tend to a Gaussian of width inversely proportional to the substrate period, giving an incoherent addition of the individual gratings and a resolution that depends on the number of layers in the coating. The size of the phase errors and their effects calls for further investigation.

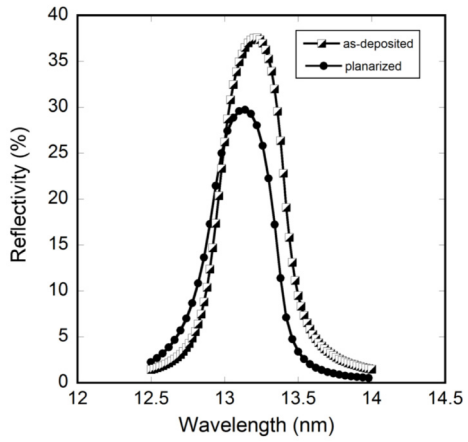

Fig. 8. Reflectivity curves as a function of wavelength of the 3,200-bilayer multilayer coated on the blazed grating substrate before (squares, as-deposited) and after (circles, planarized) polishing the top surface.

The EUV reflectometer of PTB at the MLS storage ring as described above was used to determine the optimum angle at which this grating should be used and its efficiency. The multilayer in this study was designed to reflect at 6° off normal ($\theta_B = 84^\circ$) and the cut angle (γ) of our substrate was 10.5°. The incidence angle α and the reflected angle β are defined relative to the top surface as explained in Fig. 1. Hence, the expected incidence angle α should be −16.4° (or −4.4°) and the reflected beam angle β 4.4° (or 16.4°), with both the incident and reflected beams on the same side of the surface normal. An X-ray reflectivity map of the multilayer based grating as a function of the detector angle β and wavelength λ was measured at an incident angle $\alpha = -16.4^\circ$, and a high dispersion with the maximum performance close to 13.2 nm was demonstrated (Fig. 9).

#237670 - $15.00 USD Received 7 Apr 2015; revised 25 May 2015; accepted 26 May 2015; published 1 Jun 2015

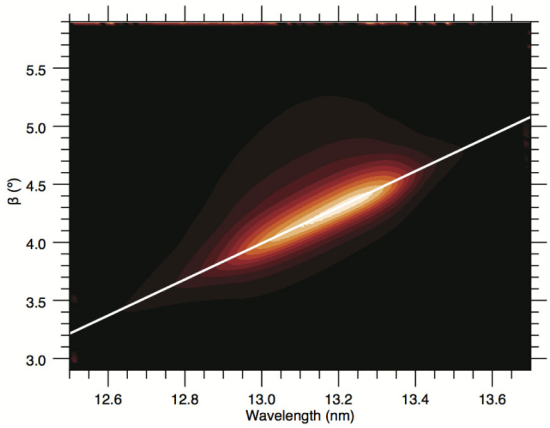

Fig. 9. Two dimensional reflectivity map showing the performance of our soft X-ray diffraction grating as a function of the detector angle β and wavelength λ at an incident angle of α = –16.4°. A high dispersion of the grating is demonstrated, as expected for a grating with 36.95 nm period. The grating equation for this period is indicated by the white line. The detector consisted of a diode behind a 4.5 × 1.0 mm^2 aperture at a 550 mm sample-detector distance, yielding an angular resolution of 0.1°. The spectral bandwidth of the beam was about 0.02 nm.

Finally, we would like to point out that the alignment precision is limiting the dimension of the blazed substrate in the <111> plane direction, the dimension within the same saw-tooth segment. The alignment, which in our case was done with the optical mask aligner, could be improved by using electron beam lithography, for example. The perpendicular direction, along the X-ray beam propagation, in which the grating is used and which goes across many segments, is not as sensitive to the alignment precision

4. Conclusion

We present the fabrication and characterization of asymmetric-cut multilayer gratings, in which long-period blazed substrates are used to extend their width. The new approach overcomes the previous limitation where the grating size was determined by the maximum multilayer thickness one can make in a single deposition run. Wet anisotropic etching was developed to obtain good quality blazed grating substrates. We demonstrated the technique by fabricating an extended asymmetric-cut multilayer grating with grating frequency of 27,060 line pairs per mm and ~30% absolute efficiency. We believe that this result could be further improved by using smoother substrates and by reducing the grating dead area. This requires further development and optimization of the etching process and multilayer coating procedure, and an investigation of the substrate blazed grating geometry. In general, further development of thick multilayer coatings is essential to achieve high resolution gratings since the resolution is determined by the number of multilayer periods deposited. The capability to extend the asymmetric-cut dimension along the X-ray beam direction is very important and opens up new applications for X-ray optics at synchrotron radiation and XFEL light sources.

Acknowledgments

We would like to thank Sabrina Bolmer (DESY) for technical assistance, and Victor Soltwisch and Christian Laubis (PTB) for constructive discussions and assistance with reflectivity measurements. Funding for this project was provided by the Helmholtz Association through program-oriented funds.

#237670 - $15.00 USD Received 7 Apr 2015; revised 25 May 2015; accepted 26 May 2015; published 1 Jun 2015